Kinetic Energy of Free Electrons Affects MALDI Positive Ion Yield via Capture Cross-Section

3 AUTHORS, INCLUDING:

Vladimir Frankevich
Research Center for Obstetrics, Gynecology a…

53 PUBLICATIONS **1,269** CITATIONS

SEE PROFILE

Renato Zenobi
ETH Zurich

456 PUBLICATIONS **13,103** CITATIONS

SEE PROFILE

Kinetic Energy of Free Electrons Affects MALDI Positive Ion Yield via Capture Cross-Section

Maxim Dashtiev, Vladimir Frankevich,[†] and Renato Zenobi*

Department of Chemistry and Applied Biosciences, ETH Zurich, CH-8093 Zürich, Switzerland

Received: June 21, 2005; In Final Form: November 16, 2005

A method for enhancing positive analyte ion signal in MALDI is described. The idea is based on influencing the kinetic energy of free electrons emitted from the organic/metal interface. It has been recently shown that free electrons in MALDI have energies around 1 eV. This energy is close to the maximum capture cross-section of most common MALDI matrices, leading to the efficient formation of negative matrix ions. This results in the reduction of the positive analyte ion yield. The effect can be minimized by shifting the kinetic energy of the electrons away from the maximum of the matrix capture cross-section by choosing a different substrate material.

Introduction

Since its invention, matrix-assisted laser desorption/ionization mass spectrometry (MALDI) has become a powerful technique for studying biological molecules and polymers.[1−3] MALDI is a soft ionization method, i.e., little or no fragmentation occurs, which makes identification of intact molecules straightforward. There are numerous open questions about how to optimize MALDI parameters to increase the ion yield or the shot-to-shot reproducibility. It is well-known that the ion yield in MALDI is very low, on the order of 10^{-4}.[4,5] A better understanding of the ionization/desorption mechanisms is required to explain various processes responsible for ion formation in MALDI. Several models of ion formation have been proposed for MALDI,[6−8] and a number of experimental approaches have been suggested toward signal enhancement, including improved sample preparation and proper choice of matrix/analyte ratio.[9−11] Significant signal improvements were found when various special MALDI targets were used.[12−16] In one example, a sample support coated with a thin layer of Teflon that carries an array of 200-μm gold spots was used, which provides hydrophilic anchors for the sample. The detection sensitivity for several standard peptides was increased to 100 amol.[15] In another example, a thin film of paraffin attached to a standard stainless steel sample support was employed for the analysis of DNA.[13] The authors showed a fivefold decrease in detection limits, as well as improvement of the shot-to-shot and sample-to-sample reproducibility. In similar research on tryptic peptides, a hydrophobic coating based on 3M Scotch Gard on the MALDI plate results in spot size reduction and increased detection sensitivity.[14] However, often the explanations for these effects are either not fully described in the literature or not based on any physical effects. In most cases, a smaller sample spot size and thus a higher local concentration of the analyte in a spot was the only reason given for the improvement in sensitivity.

Recently, the effects of the sample preparation and of the target material were interpreted in a new fashion:[17] it was found that a substantial number of photoelectrons are emitted from the metal target[18,19] under laser irradiation, when only a thin MALDI sample is present. It was already suspected by Karas and co-workers[20] that electrons play a role in MALDI, although these workers assumed that electrons originate only from matrix photoionization (in the case of positive ions) or from reaction with protonated matrix species (in case of negative ions). The presence of electrons may play a major role in suppressing positive ion signal of analytes as well as decreasing detection limits. In work from this laboratory,[17] an increase by more than 2 orders of magnitude of positive ion signal of bovine serum albumin and bradykinin was demonstrated when electron photoemission was absent; a substantial improvement in mass resolution was also achieved.

In this work, we take a closer look at the photoelectrons emitted from a MALDI target. We found that electrons with particular kinetic energies are primarily responsible for reducing the positive ion signal. A way to influence the electron energy and to increase positive analyte signal is discussed.

Experimental Section

The experiments were performed on a Fourier transform ion cyclotron resonance (FT-ICR) mass spectrometer that consists of a home-built vacuum system, a 4.7 T superconducting magnet (Bruker, Fällanden, Switzerland), and commercial control electronics and data acquisition (IonSpec Corp., Lake Forest, CA). A home-built open cylindrical cell was used for trapping the ions. The instrument has an internal MALDI source with a target that was positioned 2 cm from the cell. For laser desorption/ionization, the third harmonic of a Nd:YAG laser (Continuum, Minilite ML-10, U.S.A.) at 355 nm with a 5-ns pulse width was used. The laser spot diameter was 900 μm. Experiments were performed both in negative and in positive modes. Bradykinin was purchased from Bachem AG (Switzerland), α-cyano-4-hydroxycinnamic acid (HCCA, purity 99%) from Sigma (Switzerland), 2,5-dihydroxybenzoic acid (DHB, purity 99%) from Acros Organics (New Jersey, U.S.A.), and

---

* To whom correspondence should be addressed. E-mail: zenobi@org.chem.ethz.ch. Tel: +41 (44) 632-43-76. Fax: +41 (44) 632−12−92.
† Current address: Institute for Energy Problems of Chemical Physics, Russian Academy of Sciences, Moscow.

MALDI Positive Ion Yield

J. Phys. Chem. A, Vol. 110, No. 3, 2006 **927**

sulfur hexafluoride from Aldrich (Buchs, Switzerland). HCCA was dissolved in a buffer containing 80% acetonitrile (ACN), 0.1% trifluoroacetic acid (TFA), and 20% water. DHB was dissolved in methanol. Both HCCA and DHB were used without further treatment or purification. MALDI samples were prepared using a standard "dried droplet" method at a matrix/analyte concentration ratio of 100:1. Spectra were obtained by averaging over a large area, with the laser beam being scanned continuously and randomly over the sample. Typically, 50 scans were co-added for each measurement. The mean of multiple measurements was taken for each data point. To determine the error bars of the data, one standard deviation from the mean was calculated. The standard deviation of the peak intensities was determined experimentally to be in the range 15−20% for all MALDI and electron capture experiments.

Stainless steel and nickel sample supports were machined in-house, and a gold support was made by vapor deposition of a 300-nm gold layer onto a standard stainless steel support. The deposition of gold was performed in-house on a commercial coating machine (MED 020, Bal-Tec, Liechtenstein). Light microscope images were taken on a standard instrument (BH2, Olympus) with reflected light illumination.

Electrons cannot be directly measured in a FT-ICR cell because of their high cyclotron frequency. SF_6 buffer gas was therefore used to detect free electrons indirectly. It is well-known that SF_6 is an efficient electron scavenger with a maximum cross-section at an electron energy close to 0 eV.[12] Higher kinetic energy electrons are captured after inelastic scattering of electrons from SF_6 gas molecules. The number of SF_6^- ions is thus proportional to the total number of electrons emitted from the MALDI target. The SF_6^- was introduced into the ICR cell through a leak valve (RME 005, Pfeiffer Vacuum, Switzerland) to a pressure of 1×10^{-6} Torr. Ions and electrons produced upon laser irradiation drifted into the field-free region of the open cell and became trapped using gated trapping with a potential well of 10 V. After an appropriate delay time, all ions of the selected polarity were excited by chirp excitation and detected.

The experimental data in Figure 2 were fitted by both linear ($y = ax$) and quadratic ($y = ax^2$) functions, using commercial software (Igor Pro V4.08, Wavemetrics, Lake Oswego, OR). The coefficients of the fitted curves were calculated on the basis of minimizing the value of the chi-square (χ^2). χ^2 is defined as $\Sigma_i[(y - y_i)/\sigma_i]^2$ where y is a fitted value for a given point, y_i is the measured data value for the point, and σ_i is an estimate of the standard deviation for y_i. All fits were restricted to go through the origin, because no photons will yield no electrons and no SF_6 ion signal; simply fitting the data points with linear or quadratic functions would sometimes lead to a finite intercept, which is, of course, incorrect.

Results and Discussion

Figure 1 shows microscope images of DHB deposited on stainless steel and gold substrates, respectively. The close similarity of the crystal morphology on both gold and stainless steel substrates suggests that sample morphology does not affect the ionization process of the sample. Therefore, significant changes in ion signal intensity due to the morphology of the sample are unlikely. The spaces between the crystal needles of DHB are relatively large, and the underlying metal surface will always be exposed to the laser beam. Thus, the emission of photoelectrons from the organic/metal interface will be possible from all such samples.
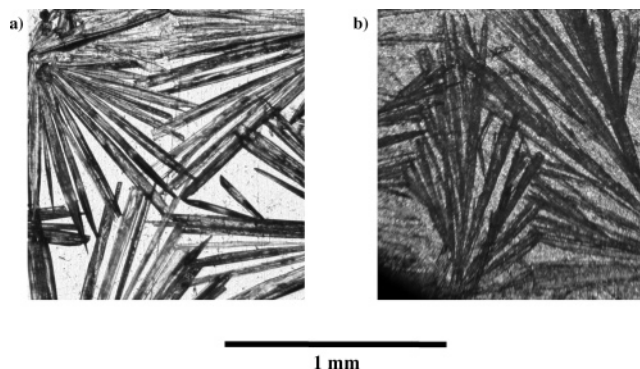

Figure 1. Light microscope images of 2,5-dihydroxybenzoic acid (DHB) crystallized on (a) a stainless steel substrate and (b) a gold substrate. The typical needlelike crystal morphology of DHB is observed on both substrates. The difference in constrast is an artifact due to differences in the illumination conditions. The spaces between crystal needles result in the underlying metal surface being exposed to the laser beam, which has a diameter of 900 μm. Therefore, production of photoelectrons from the organic/metal interface should always be possible.

The work function for nickel is 5.04 eV, for stainless steel is ∼4.6 eV, and for gold is 5.1 eV. The photon energy corresponding to the third harmonic of a Nd:YAG laser is 3.49 eV. Thus, we do not expect photoelectrons from pure metals due to laser irradiation. However, it has been demonstrated that the presence of an organic layer on a metal surface leads to an intense electron emission from the metal/organic interface.[17−19] This effect can be rationalized to result from the reduction of the metal work function.[21] For a single-photon process, a linear dependence of the electron yield on laser pulse energy is expected. An alternative explanation is based on the idea that matrix−analyte complexes may exhibit ionization potentials lower than that of the pure matrix, enabling two-photon ionization by typical MALDI lasers (N_2 laser, 337 nm, or tripled Nd:YAG, 355 nm).[22] In this case, a quadratic dependence on laser pulse energy would be expected.

It has been shown recently[17] that emission from a stainless steel plate covered by a thin layer of an organic matrix has a roughly linear dependence on the laser pulse energy in the range of laser energies up to 0.25 mJ (8 MW/cm²), although this has been challenged.[22] For this reason, the dependence of photoelectron emission of different metals such as nickel, stainless steel, and gold covered by a thin layer of DHB was carefully investigated in the present work. As mentioned in the experimental part, electrons can be detected by measuring the SF_6^- ion signal. Figure 2 shows the SF_6^- signal intensity versus laser energy for stainless steel (a), gold (b), and nickel (c). As clearly seen from the fits in Figure 2, the linear dependence fits better for all metals studied, thus supporting a one-photon process for photoemission. While a one-photon process is the simplest and most straightforward explanation of these data, alternative scenarios are possible: for example, deviation from quadratic behavior would be expected for a two-photon process if saturation occurs; however, this usually does not lead to a clean linear power dependence. Also, a composite model including sequential two-photon ionization of matrix in parallel with excited-state energy pooling has been proposed,[22] which did not yield a quadratic power dependence.

Because a metallic MALDI target can be a source of electrons, the presence of these electrons in the MALDI plume can affect the positive ion yield and can lead to a predominance of negative ions. The interaction of electrons with matrix ions
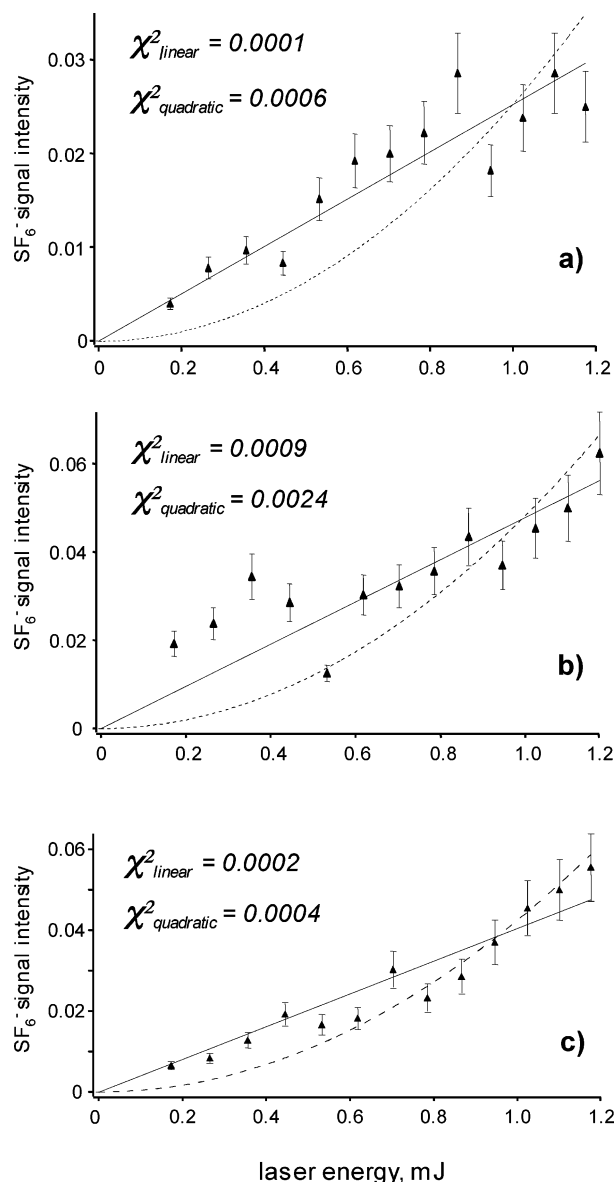
Figure 2. SF_6^- ion signal as a function of laser energy ($\lambda = 355$ nm) due to electron emission from (a) stainless steel, (b) gold, and (c) nickel. The dashed line is a quadratic function fit ($y = ax^2$), and the solid line is a linear function fit ($y = ax$). χ^2 is defined as $\Sigma_i[(y - y_i)/\sigma_i]^2$ where y is a fitted value for a given point, y_i is the measured data value for the point, and σ_i is an estimate of the standard deviation for y_i. In all cases, the data is better represented by a linear fit, supporting a one-photon process for electron emission.

in a MALDI plume has been suggested to occur by the following reaction:[17]

$$M + e^- \rightarrow [M - H]^- + H^\bullet \qquad (1)$$
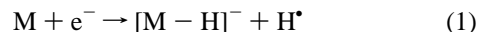
Electron capture by M has a cross-section that varies with the kinetic energy of the electrons. In the work by Asfandiarov et al.,[23,24] electron capture cross-sections for typical MALDI matrices were measured. In their work, the investigated molecules were irradiated by electrons of controlled energy (0−10 eV) in a vacuum of 10^{-4} Torr, and the electron capture cross-section was plotted as a function of the incident electron energy. These authors found that the maximum cross-sections for DHB, sinapinic acid, and nicotinic acid are around 1 eV; for caffeic acid, it is 0.6 eV; and for HCCA, it is around 0.2 eV. As an example, the measurement of the capture cross-section for DHB vs electron energy, taken from ref 23, is shown in Figure 3.
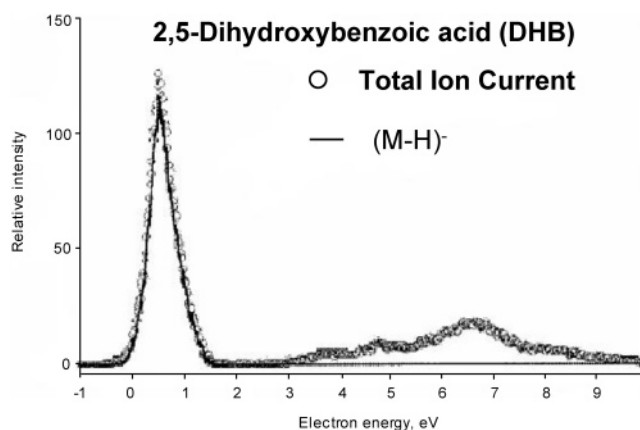
Figure 3. Plot of the electron capture cross-section of DHB, showing the total negative ion current (circles) and the ion current of deprotonated DHB, $[M - H]^-$, vs incident electron energy. The resonance at 0.85 eV is clearly observed. Reproduced with permission from ref 23, copyright ISI publications.

The maximum of the capture cross-section is observed at around 0.85 eV. In this work, the two of the most widely used MALDI matrices, DHB and HCCA, were employed.

Following formation of $[M - H]^-$, negative matrix ions can further interact with positive analyte ions in the plume, leading to suppression of the positive ion signal

$$[M - H]^- + AH^+ \rightarrow [M - H] + AH \qquad (2)$$

In our FT-ICR setup, the sample substrate was directly connected to a voltage. We were thus able to control the kinetic energy of electrons by applying different voltages to the substrate. This, in turn, allowed us to control the number of negative matrix ions produced, affecting the rate of reaction 1. Although this is technically rather difficult to implement, and the energy of the analyte ions is also affected by changing the kinetic energy of the electrons, it is the reaction of the electrons with neutral matrix molecules, which is of primary interest here. Control of the rate of reaction 1 is possible not only by applying a voltage to the MALDI plate, but also by changing the material of the plate (work function). In the work of Gorshkov et al.,[19] the electron energy distribution for stainless steel and gold was measured. It was found that the maxima for stainless steel and gold are around 1 and 0.55 eV, respectively. Thus, by substituting the stainless steel plate with gold, the electron energy is changed from 1 to 0.55 eV. For DHB, this results in a shift away from the maximum capture cross-section. In Figure 4a, the negative-mode mass spectrum of DHB deposited on a stainless steel sample support is shown. The most abundant peak is 153 Da corresponding to $[M - H]^-$, which is formed by electron capture dissociation. Figure 4b shows the mass spectrum of the same compound deposited on a gold plate. It can be seen that the peak at 152 Da, corresponding to $[M - H_2]^-$, is predominant in this spectrum. This fragment has already been observed by other research groups,[20,25] but its origin is not completely clear yet. It has been shown by Bourcier[25] that the 152 Da fragment appears only above a laser pulse energy of 19 μJ. A similar observation was reported by Karas[20] et al. In normal MALDI as well as on the gold substrate, we propose that the 152 Da peak is formed by the loss of a hydrogen radical from the deprotonated DHB, resulting in a cyclic resonance structure that involves the carboxyl group and the hydroxyl group in position 2. On the stainless steel substrate, the energy of the emitted photoelectrons is in resonance with the maximum capture cross-section of DHB, i.e., electron capture rather than

MALDI Positive Ion Yield

J. Phys. Chem. A, Vol. 110, No. 3, 2006 **929**
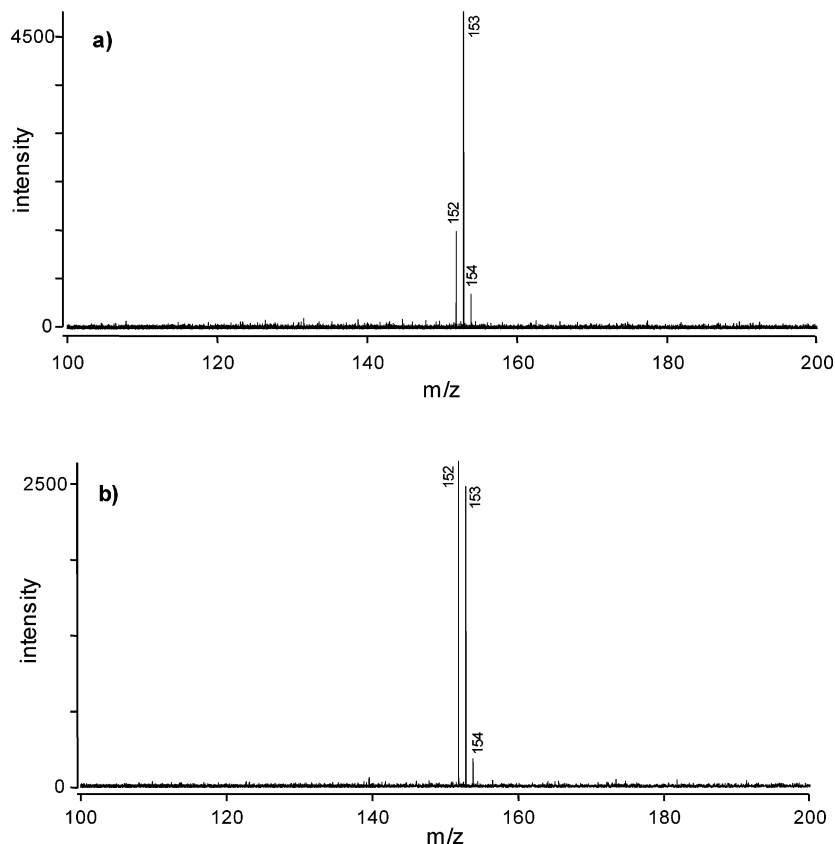
Figure 4. Negative-mode MALDI mass spectra of 2,5-dihydroxybenzoic acid (DHB) deposited on (a) a stainless steel plate and (b) a gold plate. The decreased number of $[M - H]^-$ ions in the case of the gold substrate slows the rate of reaction 2, thus preventing the neutralization of positive analyte ions. Standard deviation of the MALDI peak intensities was 15−20%.

deprotonation will be the dominant process. Electron capture can take place on every electronegative atom of DHB, and subsequent loss of a hydrogen radical is expected to be the pathway for formation of $[M - H]^-$. The reaction to $[M - H_2]^-$ will not necessarily involve the adjacent carboxyl and 2-OH groups, i.e., the formation of the stabilized cyclic resonance structure is less probable. In many instances, the $[M - H]^{\bullet-}$ at $m/z = 153$ will thus survive.

The key result obtained from the data in Figure 4 is that the negative ion yield is greatly decreased when going from stainless steel to gold, by about a factor of 2. This is interpreted to be a direct result of a lower capture cross-section, as the kinetic energy of the electrons is shifted from its maximum at 1 eV (stainless steel) to 0.55 eV (gold). Shifting the electron energy from the maximum changes the rate of reaction 1. Our interpretation is that decreasing the number of negative matrix ions in the MALDI plume will decrease the total number of negative charges in the plume and prevent the neutralization of positive analyte signal.

In the case of HCCA, the energy of photoelectrons emitted from either stainless steel or gold does not coincide with the capture cross-section maximum of HCCA. However, it was found[24] that the formation of the main fragment $[M - CO_2]^-$ has a maximum at an electron energy of 0.5 eV in negative ion mass spectrometry. This energy corresponds almost exactly to the energy of photoelectrons emitted from gold. Figure 5 shows a negative-mode mass spectrum of HCCA deposited on stainless steel and gold. As can be clearly seen in Figure 5b, the formation of $[M - CO_2]^-$ is a predominant process on the gold plate.

Figure 6 shows the spectrum of bradykinin on stainless steel (a) and gold (b) plates. All the experimental conditions such as laser power, sample preparation, analyte concentrations, and so
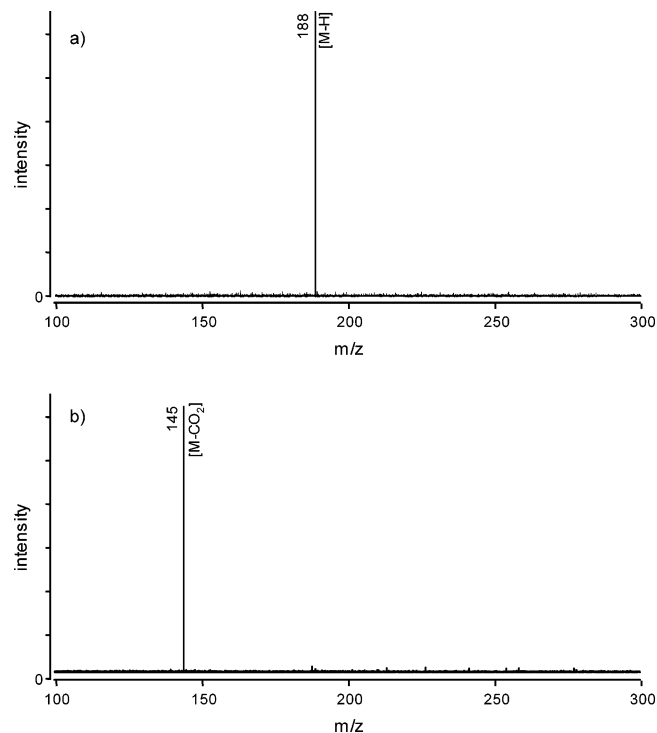
Figure 5. Negative-mode MALDI mass spectra of α-cyano-4-hydroxycinnamic acid (HCCA) deposited on (a) a stainless steel plate and (b) a gold plate. Standard deviation of the MALDI peak intensities was 15−20%. Since the formation of the $[M - CO_2]^-$ fragment peaks at an electron energy of 0.5 eV, and the kinetic energy of photoelectrons emitted from gold is around 0.55 eV, the intensity of the $[M - CO_2]$ fragment it is more pronounced on the gold substrate.
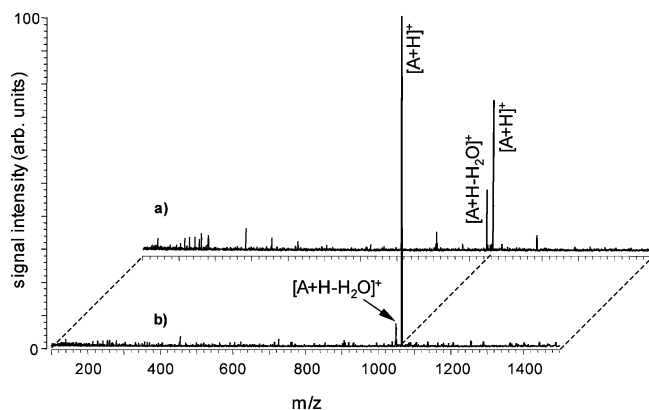
Figure 6. Positive-mode MALDI mass spectrum of bradykinin with DHB as a matrix, deposited on (a) a stainless steel plate and (b) a gold plate. Standard deviation of the MALDI peak intensities was 15−20%. An increase by a factor of about 2 is demonstrated on the gold substrate.

forth were identical. An increase by a factor of 2 in ion intensity for gold is demonstrated. On the basis of the above considerations, it is straightforward to understand this increase. As found before, the average electron energy from the gold plate is 0.55 eV; thus, reaction 1 is ineffective, and many fewer negative matrix ions are present in a MALDI plume. As a result, the rate of reaction 2 will be lowered as well.

It should be noted that the signal enhancement is not as dramatic as in the case of nonmetallic targets. In the experiments presented here, we influence the charge balance of the MALDI plume only by shifting the kinetic energy of the electrons away from the maximum cross-section for negative ion formation. However, this does not stop reaction 1 completely.

Conclusions

The laser energy dependence of photoelectron emission from MALDI samples deposited on stainless steel, gold, and nickel was investigated. The results obtained support a one-photon model for photoemission, as proposed in ref 17. The substrate material was shown to play an important role in the MALDI process. By choosing different substrates, we were able to manipulate the photoelectron kinetic energy, and, by virtue of the energy-dependent capture cross-section of the matrix,

decrease the number of negative matrix ions, which led to an increase in analyte signal in positive ion mode.

References and Notes

(1) Karas, M.; Bachmann, D.; Bahr, U.; Hillenkamp, F. *Int. J. Mass Spectrom. Ion Processes* **1987**, *78*, 53.

(2) Karas, M.; Bachmann, D.; Hillenkamp, F. *Anal. Chem.* **1985**, *57*, 2935.

(3) Karas, M.; Hillenkamp, F. *Anal. Chem.* **1988**, *60*, 2299.

(4) Mowry, C. D.; Johnston, M. V. *J. Phys. Chem.* **1994**, *98*, 1904.

(5) Puretzky, A. A.; Geohegan, D. B. *Chem. Phys. Lett.* **1998**, *286*, 425.

(6) Zenobi, R.; Knochenmuss, R. *Mass Spectrom. Rev.* **1998**, *17*, 337.

(7) Fournier, I.; Brunot, A.; Tabet, J. C.; Bolbach, G. *Int. J. Mass Spectrom.* **2002**, *213*, 203.

(8) Karas, M.; Krüger, R. *Chem. Rev.* **2003**, *103*, 427.

(9) Dai, Y.; Li, L.; Roser, D. C.; Long, S. R. *Rapid Commun. Mass Spectrom.* **1999**, *13*, 73.

(10) Dai, Y. Q.; Whittal, R. M.; Li, L. *Anal. Chem.* **1999**, *71*, 1087.

(11) Wang, Z. P.; Russon, L.; Li, L.; Roser, D. C.; Long, S. R. *Rapid Commun. Mass Spectrom.* **1998**, *12*, 456.

(12) Christophorou, L. G.; Olthoff, J. K. *J. Phys. Chem. Ref. Data* **2000**, *29*, 267.

(13) Hung, K. C.; Rashidzadeh, H.; Wang, Y.; Guo, B. *Anal. Chem.* **1998**, *70*, 3088.

(14) Owen, S. J.; Meier, F. S.; Brombacher, S.; Volmer, D. A. *Rapid Commun. Mass Spectrom.* **2003**, *17*, 2439.

(15) Schürenbeg, M.; Lübbert, C.; Eickhoff, H.; Kalkum, M.; Lehrach, H.; Nordhoff, E. *Anal. Chem.* **2000**, *72*, 3436.

(16) Yuan, X. L.; Desiderio, D. M. *J. Mass Spectrom.* **2002**, *37*, 512.

(17) Frankevich, V. E.; Zhang, J.; Friess, S. D.; Dashtiev, M.; Zenobi, R. *Anal. Chem.* **2003**, *75*, 6063.

(18) Frankevich, V.; Knochenmuss, R.; Zenobi, R. *Int. J. Mass Spectrom.* **2002**, *220*, 11.

(19) Gorshkov, M. V.; Frankevich, V. E.; Zenobi, R. *Eur. J. Mass Spectrom.* **2002**, *8*, 67.

(20) Karas, M.; Glückmann, M.; Schafer, J. *J. Mass Spectrom.* **2000**, *35*, 1.

(21) Seki, K.; Hayashi, N.; Oji, H.; Ito, E.; Ouchi, Y.; Ishii, H. *Thin Solid Films* **2001**, *393*, 298.

(22) Knochenmuss, R. *Anal. Chem.* **2004**, *76*, 3179.

(23) Asfandiarov, N. L.; Pshenichnyuk, S. A.; Fokin, A. I.; Lukin, V. G.; Fal'ko, V. S. *Rapid Commun. Mass Spectrom.* **2002**, *16*, 1760.

(24) Pshenichnyuk, S. A.; Asfandiarov, N. L. *Eur. J. Mass Spectrom.* **2004**, *10*, 477.

(25) Bourcier, S.; Bouchonnet, S.; Hoppilliard, Y. *Int. J. Mass Spectrom.* **2001**, *210*, 59.